Arthritis & Rheumatism
DOI 10.1002/art.38199

Title: Protective effects of C-type natriuretic peptide on linear growth and articular cartilage integrity in an inflammatory arthritis mouse model.

Short title: C-type natriuretic peptide protects cartilage during arthritis

Hülya Bükülmez, MD.[1], Fozia Khan, PhD.[2], Cynthia F. Bartels, MS.[3], Shunichi Murakami MD., PhD.[4], Adriana Ortiz-Lopez, PhD.[5], Abdus Sattar, PhD.[6], Tariq M. Haqqi, PhD.[7], Matthew L. Warman, MD.[8]

Corresponding author: Hülya Bükülmez, MD, Skeletal Research Center, Department of Biology, College of Arts and Sciences and Pediatric Rheumatology, and Department of Pediatrics, MetroHealth Medical Center, Case Western Reserve University School of Medicine, Cleveland, OH,

Address: Department of Pediatrics, Pediatric Rheumatology, 2500 MetroHealth Drive, Cleveland, OH, 44106. Tel: 216-778-4284, Fax: 216-778-2857, e-mail: hxb38@case.edu,

Supported by grants from the Arthritis National Research Foundation and from NIH/NIAMS K08 AR053943-01, and from NIH/NCCAM R01 AT 0036227; R01 AT 005520; and R21 AT 004026.

Authors do not have any financial supports from commercial sources, thus no conflicts of interest.

Received: Nov 21, 2011; Revised: Jul 30, 2013; Accepted: Sep 12, 2013

Abstract:

Objective: The C-type natriuretic peptide (CNP) signaling pathway is a major contributor to post-natal skeletal growth in humans. In this study we investigated whether CNP signaling could prevent growth delay and cartilage damage in an animal model of inflammatory arthritis.

Methods: We generated transgenic mice that overexpress CNP *(B6; SJL* $Tg^{Col2a1\text{-}NPPC}$*)* in chondrocytes. We introduced the CNP transgene into an animal model of systemic inflammatory arthritis (K/BxN TCR) and determined the effect of CNP overexpression in chondrocytes on arthritis severity, cartilage damage, and linear growth. We also examined primary chondrocyte cultures for gene and protein expression changes that result from CNP overexpression.

Results: K/BxN TCR mice exhibited linear growth delay (p<0.01) compared to controls and their growth delay correlated with arthritis severity. K/BxN TCR mice also had diminished chondrocyte proliferation and matrix production. Compared to non-CNP transgenic mice, K/BxN TCR mice that overexpress CNP had milder arthritis, no growth delay, and less cartilage damage. Primary chondrocytes from CNP overexpressing mice were less sensitive to inflammatory cytokines than wild-type chondrocytes.

Conclusion: CNP overexpression in chondrocytes can prevent endochondral growth delay and protect against cartilage damage in a mouse model of inflammatory arthritis. Pharmacologic or biologic modulation of the CNP signaling pathway may prevent growth retardation and protect cartilage in patients with inflammatory joint disease, such as juvenile idiopathic arthritis (JIA).

Introduction:

Linear growth results from the action of multiple signaling pathways. The pathway that includes C-type Natriuretic Peptide (CNP) contributes to chondrocyte proliferation, differentiation, and matrix synthesis in skeletal growth plates (1) (2) (3) (4). Patients with homozygous loss-of-function mutations in the CNP receptor Natriuretic Peptide Receptor B (NPR-B) have Acromesomelic Dysplasia (5) and heterozygous mutation carriers frequently have short stature (6). Also, patients with chromosome translocations that cause CNP overexpression develop skeletal overgrowth (7). These conditions point toward a dose dependent effect of CNP signaling on linear growth. Therefore, linear growth may be affected in patients with acquired diseases that alter the production of CNP or the expression of its receptor NPR-B.

Children with Juvenile Inflammatory Arthritis (JIA) have impaired linear growth, and 40% percent of children with JIA develop bone degeneration and deformity adjacent to affected joints (8-11). The mechanism by which chronic systemic inflammation suppresses linear growth in children with JIA is not completely understood (12, 13). Alterations in the growth hormone (GH) and the insulin-like growth factor (IGF) signaling pathways have been associated with growth delay in children with chronic arthritis (14). Although serum GH levels were unchanged in patients with JIA, patients did have reduced levels of IGF1 and IGF binding protein-3 (IGFBP3) suggesting that inflammation causes GH resistance. The CNP signaling pathway has not been studied in children with JIA.

Animal models of inflammatory arthritis have been used to delineate pathways that contribute to impaired linear growth and joint deformity (15). Local elevations of

TNF-α, IL-6, and IL-1 β levels have been observed in affected growth plates. Furthermore, overexpression of IL-6 (16) or TNF-α (17) in transgenic mice causes systemic inflammatory arthritis and growth retardation. By 25 days of age the K/BxN TCR mouse model exhibits pronounced joint inflammation that resembles rheumatoid arthritis (RA) (17-19). Here, we report that the K/BxN TCR mouse model develops linear growth delay and cartilage damage that can be lessened by overexpression of CNP in chondrocytes.

Materials and Methods

These experiments were approved by the Institutional Animal Care and Use Committee at Case Western Reserve University.

Generation of CNP transgenic mice: We cloned the full-length human CNP (NPPC) cDNA into the pKN185 vector, which drives CNP expression under the control of mouse collagen type II (*Col2a1*) promoter and enhancer (20).Transgenic animals ($Tg^{Col2a1\text{-}NPPC}$) were produced following pronuclear injection into zygotes on a mixed SJL/C57BL/6J background. One founder that had ~ 4 copies of the CNP transgene integrated into a single locus, as determined by Southern blotting and Mendelian segregation of the transgene, was then backcrossed for >20 generations onto the C57BL/6J background.

Development of K/BxN TCR arthritis mouse model: KRN T-cell receptor (TCR) transgenic mice (K/B/6 TCR), as well as K/BxN TCR mice that develop spontaneous arthritis, have been previously described (21-23). K/B/6 TCR mice were a gift from Mathis and Benoist Laboratories (Joslin Diabetes Center, Harvard Medical School). K/BxN TCR mice were obtained by crossing K/B/6 TCR transgenic mice with non-obese diabetic (NOD/ShiLTj) mice. NOD/ShiLTj mice were obtained from Jackson

Laboratories. Only offspring that inherit the TCR transgene develop inflammatory arthritis on this background; Mice that do not inherit the TCR transgene serve as non-transgenic controls (NOD/B/6 or BxN in figure 3A).

Breeding the CNP transgene into the arthritis model: We bred mice with $Tg^{Col2a1\text{-}NPPC}$ to KRN TCR mice. Offspring that carried both the $Tg^{Col2a1\text{-}NPPC}$ and the TCR transgenes were then bred with NOD mice. The phenotypes of offspring that were double heterozygous for the TCR and $Tg^{Col2a1\text{-}NPPC}$ transgenes (K/BxN TCR; $Tg^{Col2a1\text{-}NPPC}$) were compared to the phenotypes of offspring that only inherited the TCR transgene (K/BxN TCR). K/BxN TCR mice will be shown as K/BxN mice for brevity in the following figures. Other offspring resulting from this cross included mice heterozygous for only $Tg^{Col2a1\text{-}NPPC}$ and mice that inherited neither transgene (BxN). Offspring were examined at birth and then examined weekly from 3 weeks until 20 weeks of age.

Small Animal X-ray Imaging: A Faxitron Radiographic Inspection Unit, (Model 8050-010, Field Emission Corporation McMinnville, OR) was used to obtain X-ray images of the mice *post mortem*. Legs were exposed for 1.5 min at 35 kVp; the entire body was exposed for 1.5 min at 30 kVp.

Clinical scoring of arthritis severity: The severity of clinical arthritis was determined using a previously described scoring system (24, 25) with modifications as described in Supplemental Table 1. Higher scores indicate increased severity of clinical arthritis.

Sample collection: Mice were terminally bled under sedation and then euthanized. Samples were collected from mice that were 1, 2, 3, 4, 6, 8, 12, 16, and 24 months old. To evaluate the growth plates, one hind leg (femur and tibia) from each mouse was

dissected, fixed with 4% formaldehyde in phosphate-buffered saline (PBS) for 24 hours at 4˚C, decalcified with 0.5 M EDTA for 1 week and then embedded in paraffin. Four µm coronal sections across the femoro-tibial joint were stained with Safranin-O/fast green or Hematoxylin & Eosin (H&E) and used for immunohistochemical staining or for *in situ* hybridization. For accurate measurement of articular cartilage and growth plate cartilage, sections were obtained at the level of anterior cruciate ligament insert into the tibia.

Histological scoring system: Histological evaluation of knee joint inflammation and cartilage integrity was performed using two scoring systems. 1) The histological scoring system of Pettit et al. (2001) was used to assess the severity of inflammatory arthritis (26). The International Cartilage Repair Society (ICRS) scoring system was used to assess the status of the extracellular matrix repair in joint cartilage (Supplemental Table 2) (27). A blinded investigator (JFW) who was not a part of the study performed the scoring of the unidentified mouse knee sections.

Cell proliferation analysis by BrdU labeling: BrdU (Zymed) was injected intra peritoneal at a dose of 300 mg/kg. Mice were sacrificed 2 h after injection. Tissue was processed and paraffin-embedded as described above. BrdU incorporation was detected using a BrdU-staining kit (Zymed) following the manufacturer's recommendation. The percentage of BrdU-positive cells was determined by dividing the number of BrdU-positive chondrocytes by the total number of chondrocytes that were counted in multiple sections of the growth plate.

***In situ* hybridization**: Slides were deparaffinized and fixed in 4% formaldehyde. Sections were digested with proteinase K (1 µg/ml) for 20 min at 37°C, and acetylated in 0.25% acetic anhydride in 0.1 M triethanolamine-hydrochloride. After re-fixation in 4% formaldehyde, sections were hybridized with ^{35}S-labeled riboprobes in hybridization buffer (50% deionized formamide, 300 mM NaCl, 20 mM Tris–HCl, pH 8.0, 5 mM EDTA, 0.5 mg/ml yeast tRNA, 10% dextran sulfate, and 1x Denhardt's solution) in a humidified chamber at 55°C overnight. After hybridization, slides were washed with 5x SSC at 50°C, 50% formamide, 2x SSC at 65°C and 1x NTE (0.5 M NaCl, 10 mM Tris–HCl, pH 8.0, 5 mM EDTA) at 37°C then treated with RNase A (20 µg/ml) and RNase T1 (1 U/µl) in 1× NTE at 37°C for 20 min. Slides were further washed in 1x NTE at 37°C, 50% formamide, 2x SSC at 65°C, 2x SSC, 0.1x SSC, and then dehydrated with graded concentrations of ammonium acetate and ethanol. Slides were dipped in NTB emulsion (Kodak) and exposed to the emulsion for 6 weeks. Slides were developed and counterstained with Hoechst 33258 (Sigma). The *NPPC* probe was made from the PKN-hCNP vector that was originally used to create the transgenic mouse. A 5' 280-bp fragment of the human CNP cDNA sequence plus 118-bp of upstream vector sequence was used for sense and anti-sense probes (398-bp).

Primary chondrocyte isolation and cytokine treatment: Primary chondrocytes from rib cages of ~5-day-old mice were isolated by enzymatic digestion using standard methods (28). Briefly, rib cages were collected in sterile PBS. The ribs were rinsed several times before digestion with 10 ml of 3 mg/ml collagenase B (Worthington Biochemical Corporation) in DMEM medium for ~ 1 h at 37°C. The ribs were then washed several times with PBS and digested overnight at 37°C with collagenase

solution (2 ml of 3 mg/ml collagenase B/DMEM medium + 10 ml DMEM with 10% fetal bovine serum). The next day, the cell suspension was strained and the cells were pelleted at 1000 rpm for 10 min and then re-suspended in DMEM containing 10% fetal bovine serum, penicillin (100 units/ml), streptomycin (100 µg/ml), and amphotericin B (0.25 µg/ml). Viable cell counts were determined by trypan blue staining, and cells were seeded at 10^6 cells *per* 35 mm culture plate in 2.5 ml DMEM (~1.2 x 10^5 cells per cm^2). Cells were grown in culture medium until ~90% confluent, with a change of medium every three days. Once cells became ~90% confluent, chondrocyte cultures were serum-starved and treated with cytokines (10 ng/mL TNF-α or 10 ng/mL IL-1β, both from R&D Systems) overnight (18 h) and mRNA and proteins were extracted as previously described (29).

Western Blotting: Cells were lysed in 500 µl of buffer (50 mM Tris-HCl, pH 7.4; 150 mM NaCl; 1% Triton X-100; 0.1% sodium dodecyl sulfate; 0.5% sodium deoxycholate; 1 mM EDTA; 1 mM EGTA and Complete™ Protease inhibitor cocktail) and total lysate protein (60 µg/lane) was resolved by SDS-PAGE, transferred to nitrocellulose membranes (Bio-Rad), blocked with non-fat dry milk re-suspended in Tris Buffered Saline, and probed with primary and secondary antibodies as previously described (29, 30). Primary antibodies included anti-phosphorylated and anti-non-phosphorylated mitogen activated protein kinase p-38, -Erk1/2 [(MAPK-p38, phosphorylated #4631, MAPK-p38 unphosphorylated #9212, phospho-ERK 1/2/pMAPK (Thr202/Ty204) (Cell Signaling Technologies)], and anti-NPR-B (Santa Cruz Biotechnology, sc-25486). Immunoreactive proteins were visualized by using 1:1000 diluted HRP-linked secondary

antibodies and enhanced chemiluminescence (GE Healthcare, Milwaukee, WI, USA) as described (31). Secondary antibody for NPR-B was goat anti-rabbit IgG-HRP used at a dilution of 1:2000 (Santa Cruz, sc-2004).

RNA extraction and cDNA synthesis: Total cytoplasmic RNA was prepared from primary chondrocytes using the RNeasy kit (Qiagen). Two µg of RNA was reverse transcribed using a Superscript II reverse-transcriptase kit (Invitrogen, Carlsbad, CA) and the cDNA mixture was diluted 5-fold in nuclease-free water and 5 µl was used for quantitative real-time PCR (RT-PCR).

Real-time PCR: Reactions were performed in a 20 µl volume with 0.5 µM primers and SYBR Green master mix following the manufacturer's instructions (Qiagen) using the Applied Biosystems StepOnePlus thermocycler. The expression level of the housekeeping gene *Rlp7* was used to normalize mRNA expression. Primers employed to amplify specific cDNA sequences are listed in Supplemental Table 4. All reactions were performed in duplicate.

Statistics: Disease severity and histopathology scores were compared between groups, using Chi-squares for the categorical variables (clinical and histologic scores) and *t*-test for the continuous variables. Results are expressed as the mean ± SD. Analysis of variance (ANOVA) on the nose-to-tail tip length of mice was performed to test differences between the groups of mice. ANOVA F-test results were reported and *P*- values less than 0.05 were considered significant. We also used Pearson Correlation

Matrices to find correlations between the clinical and histopathology data. Statistical software SAS 9.0 and Stata 11.0 were used in analyzing the data.

Results:

$Tg^{Col2a1\text{-}NPPC}$ mice exhibit linear bone overgrowth: Mice possessing the CNP transgene driven by the *Col2a1* promoter/enhancer ($Tg^{Col2a1\text{-}NPPC}$) demonstrated skeletal overgrowth by 4 weeks of age (Supplemental Table 3). Overgrowth affected the long bones and the vertebrae (Fig. 1A, B) and was associated with increases in growth plate width, the size of hypertrophic chondrocytes [Fig. 1C, D (F test $p<0.01$)], nose-to-tail-tip length (Fig. 1E), and the number of proliferating chondrocytes (Fig. 1F) (F test $p<0.01$). The growth plate width was 148 $\pm$14 μm in $Tg^{Col2a1\text{-}NPPC}$ mice (n=12) and 99 $\pm$5.3 μm in non-transgenic controls (n=5) (Student's t-test, $p < 0.05$) at 4 weeks of age. *In situ* hybridization detected CNP transgene expression in growth plate and articular chondrocytes (Fig. 1G, H). $Tg^{Col2a1\text{-}NPPC}$ mice developed thoracic kyphosis and joint dislocations over time, but no problems outside of the skeletal system were detected.

K/BxN TCR arthritic mice exhibit linear growth delay and articular cartilage damage: K/BxN TCR mice (K/BxN in Fig. 2A) developed arthritis by 3 weeks of age and exhibited visible growth delay by 12 weeks of age when compared to littermates that did not inherit the TCR transgene (BxN) (Fig. 2A). Measurements of growth (nose-to-tail tip length) detected significant differences in linear growth between K/BxN TCR mice and BxN littermates by 4 weeks of age (Fig. 2B, F test, $p<0.01$). In order to prevent length discrepancies, we did not clip tails to obtain tissue for isolating DNA for genotyping the mice. In the K/BxN TCR mice, the severity of arthritis was inversely correlated with longitudinal growth; this correlation was strongest at 14 weeks of age (Supplemental

Fig. 1). The growth plates in K/BxN TCR mice were narrower and had fewer cells than their BxN littermates (Fig. 2C). The articular cartilage in K/BxN TCR mice also became less cellular, had less cartilage matrix, and had a more irregular surface than the BxN mice (Fig. 2D, E).

CNP overexpression in chondrocytes improves linear growth and reduces articular cartilage damage in the K/BxN TCR mice: Since CNP overexpression enhanced linear growth in wild-type mice, we sought to determine whether overexpression could protect against growth impairment in mice with inflammatory arthritis. We first bred $Tg^{Col2a1\text{-}NPPC}$ mice onto the KRN TCR background and then onto the K/BxN background (Fig. 3A).

K/BxN TCR mice that overexpressed CNP (K/BxN TCR; $Tg^{Col2a1\text{-}NPPC}$) showed no growth retardation (Fig. 3B, F test $p<0.01$), had increased width of the growth plates (Fig. 3C and Supplemental Fig. 2A), and had increased length of the long bones (Fig. 3D) compared to K/BxN TCR arthritic mice. The increase in growth plate width in mice with $Tg^{Col2a1\text{-}NPPC}$ was associated with an increase in BrdU incorporation (Supplemental Fig. 2B). CNP overexpression reduced the clinical arthritis score in the K/BxN TCR mice, with CNP overexpressing mice having an average arthritis score of 4.37 ±1.38 (n=8) compared to the K/BxN TCR average score of 8.66 ±3.26 (n=14) (t-test, $p<0.05$).

CNP overexpression also reduced the severity of articular cartilage inflammation and damage in the K/BxN TCR inflammatory mouse model (Fig. 3E). Thirteen week-old male CNP overexpressing mice had better articular cartilage chondrocyte distribution and organization, and cartilage matrix content, than the controls. Although CNP overexpression appeared to protect articular cartilage from damage caused by

inflammation (Fig. 4A-C) overexpression did not reduce inflammatory changes occurring in the synovia (Fig. 4D).

CNP overexpression enhances signal transduction via NPR-B and reduces the sensitivity of this signaling pathway to the pro-inflammatory cytokines TNF-α and IL-1β: We performed cGMP ELISAs, quantitative RT-PCR, and western blotting using rib cartilage primary chondrocyte cultures harvested from $Tg^{Col2a1\text{-}NPPC}$ and wild-type control mice. There was ~8-fold (+/- 0.7) higher intracellular cGMP levels in the $Tg^{Col2a1\text{-}NPPC}$ chondrocytes than in wild-type chondrocytes, confirming enhanced CNP signaling. In $Tg^{Col2a1\text{-}NPPC}$ chondrocytes, NPR-B (*Npr2*) expression was increased at the mRNA and protein levels (Fig. 5, 6A and Supplemental Fig. 3); $Tg^{Col2a1\text{-}NPPC}$ chondrocytes also had increased mRNA expression of pro-chondrogenic growth factors - vascular endothelial growth factor (*Vegf*) and transforming growth factor β1 (*Tgfb1*) - and increased expression of the major cartilage collagen (*Col2a1*) compared to wild-type chondrocytes (Fig. 5).

VEGF immunostaining showed VEGF expression in a wider region of the growth plate of $Tg^{Col2a1\text{-}NPPC}$ mice (Supplemental Fig.4). VEGF staining was found to encompass an area that surrounds not only the hypertrophic and proliferating chondrocytes, but also the trabecular bone beneath the hypertrophic chondrocytes where the blood vessels reside (Supplemental Fig. 4). In addition, as has been previously reported (32) we confirmed that MAPK p38 phosphorylation is increased and MAPK Erk1 phosphorylation is decreased in CNP overexpressing chondrocytes compared to wild type chondrocytes (2) (Fig. 6B).

Additionally, we also observed that mRNA expression of matrix metalloproteinase (MMP) -3, -9, and -13, were mildly increased in the $Tg^{Col2a1\text{-}NPPC}$ as compared to wild-type chondrocytes. (Fig. 6C).

Since the presence of the CNP overexpression in $Tg^{Col2a1\text{-}NPPC}$ mice appeared to protect articular cartilage *in vivo* from the damaging effect of inflammation, we tested the effects of treating primary chondrocytes from $Tg^{Col2a1\text{-}NPPC}$ and control mice with the pro-inflammatory cytokines TNF-α and IL-1β. TNF-α and IL-1β each significantly reduced *Npr2* mRNA expression in both $Tg^{Col2a1\text{-}NPPC}$ and wild-type chondrocytes. However, the level of *Npr2* mRNA expression in $Tg^{Col2a1\text{-}NPPC}$ chondrocytes after TNF-α or IL-1β treatment was comparable to *Npr2* expression in untreated wild-type chondrocytes (Fig. 6A).

In $Tg^{Col2a1\text{-}NPPC}$ chondrocytes, TNF-α exposure had no effect on MAPK p38 phosphorylation, whereas IL-1β reduced MAPK p38 phosphorylation (Fig. 6B). In contrast, both TNF-α and IL-1β treatments increased MAPK p38 phosphorylation in wild -type chondrocytes. The mRNA expression of the MMPs were either the same or less elevated in $Tg^{Col2a1\text{-}NPPC}$ compared to the wild-type chondrocytes following exposure to cytokines (Fig.6C, $p>0.05$).

IGF1, IGF1R, and IGFBP3 levels were reported to be diminished in serum of children affected by JIA, accounting for these children's longitudinal growth delay. In order to understand whether CNP overexpression affects *Igf1*, *Igf1r*, and *Igfbp3* mRNA expression, we performed quantitative RT-PCR using rib cartilage primary chondrocyte cultures harvested from $Tg^{Col2a1\text{-}NPPC}$ and wild-type mice. $Tg^{Col2a1\text{-}NPPC}$ primary chondrocytes did not have increased mRNA levels of *Igf1* or *Igf1r*, but did have ~ 6-7 -

fold increase in *Igfbp3* compared to wild-type chondrocytes. When exposed to TNF-α (10ng/ml) and IL-1β (10ng/ml) overnight, *Igf1* and *Igf1r* expression levels in chondrocytes were suppressed significantly in both $Tg^{Col2a1\text{-}NPPC}$ and wild-type chondrocytes. Interestingly, *Igfbp3* expression levels were not different between $Tg^{Col2a1\text{-}NPPC}$ and wild type chondrocytes exposed to pro-inflammatory cytokines; *and* remained up-regulated in the $Tg^{Col2a1\text{-}NPPC}$ chondrocytes (Supplemental Fig.5)

Earlier reports indicate that TNF-α and IL-1β inhibit chondrocyte differentiation and DNA synthesis in growth plate and costal chondrocytes by suppressing *Sox9* expression (33). It is known that CNP up regulates Sox9 expression in chondrocytic cells (34, 35). Thus, we sought to check whether CNP overexpression in $Tg^{Col2a1\text{-}NPPC}$ primary chondrocytes also up regulates Sox9 mRNA expression. Results showed that in $Tg^{Col2a1\text{-}NPPC}$ primary chondrocytes Sox9 expression is up regulated by 5-fold over wild-type chondrocytes. As expected, when chondrocytes were exposed to TNF-α (10 ng/ml) overnight, Sox9 expression was reduced in both WT and $Tg^{Col2a1\text{-}NPPC}$ chondrocytes, but in $Tg^{Col2a1\text{-}NPPC}$ chondrocytes the reduction brought the level to that of untreated wild-type expression. We suggest that CNP overexpression in $Tg^{Col2a1\text{-}NPPC}$ mice protected Sox-9 expression levels during TNF-α exposure (Fig. 6D).

Discussion:

In children with JIA, the inhibitory effects of pro-inflammatory cytokines (IL-6, TNF-α, and IL-1 β) on growth plate chondrocytes have been posited to contribute to growth suppression (36, 37). Elevation of pro-inflammatory cytokines (e.g., TNF-α, and IL-1β) in synovial fluid has also been associated with destruction of growth plates adjacent to an arthritic joint. Pro-inflammatory cytokines decrease the width of the

proliferating zone in growth plate cartilage leading to a decrease in endochondral bone growth. IL-1β reduces expression of cartilage collagens and proteoglycans (13, 38). In this study, we tested whether the growth promoting effects of the CNP/NPR-B signaling pathway would lessen the severity of growth failure and cartilage degeneration in a mouse model of inflammatory arthritis. We created a mouse that overexpresses CNP in chondrocytes causing increased chondrocyte proliferation, matrix production and hypertrophic chondrocyte size, consistent with previous reports (2). We then bred the CNP overexpression transgene into the K/BxN TCR mouse model of chronic inflammatory arthritis and observed that CNP overexpression reduced the damaging effects of chronic inflammatory arthritis on linear growth and articular cartilage.

There are several possible mechanisms by which CNP overexpression protects growth plate and articular cartilage from inflammation-induced damage. One possibility is that CNP overexpression increases chondrocyte functioning thereby blunting the consequence of the inflammatory cytokines negative effects. Interestingly, activation of MAPKs, particularly MAPK p38, is a critical event that leads to the production of several mediators of cartilage damage in an arthritic joint, including the MMPs (39). Therefore, it was surprising that CNP overexpression protected articular cartilage while also significantly increasing MAPK p38 phosphorylation. CNP signaling may favor the activation of pathways downstream of MAPK p38 that are anabolic, whereas inflammatory cytokines favor the activation of pathways that are catabolic.

Growth delay in children with JIA is suggested to be due, at least in part, to reduced levels of IGF1 and IGFBP3 Therefore, we studied the effect of CNP overexpression on *Igf1* mRNA expression in the primary chondrocytes isolated from rib

cage cartilage of $Tg^{Col2a1\text{-}NPPC}$ mice and wild-type mice using qRT-PCR. Results showed that while there was no significant suppressive effect of CNP overexpression on *Igf1* and *Igf1r*, while there was a significant increase in *Igfbp3* expression levels. In a previous human study, the authors showed that an AMDM patient lacking NPR2 function had low serum levels of IGFI. It may be possible that lack of CNP signaling negatively regulate IGF1 levels. However, AMDM patients have a skeletal dysplasia that is distinct from that seen in IGF1 deficiency. Furthermore, AMDM patients are able to produce IGF1 when a IGF1 generation test is performed (40). Our $Tg^{Col2a1\text{-}NPPC}$ mice data do not suggest any direct regulatory effects of excess CNP on IGF1 signaling pathway.

Igf1 and *Igf1r* expression were similarly suppressed in both $Tg^{Col2a1\text{-}NPPC}$ mouse primary chondrocytes and wild type chondrocytes when cultures were exposed to TNF-α (10ng/ml) and IL-1β (10ng/ml) overnight, while *Igfbp3* expression remained up regulated. But, in the absence of a significant change in *Igf1* and *Igf1r* expression in $Tg^{Col2a1\text{-}NPPC}$ mouse chondrocytes, we do not think that the cartilage protective effects of CNP are due to its regulatory effects on *Igf1* signaling.

Earlier reports have indicated that TNF-α and IL-1β inhibit chondrocyte differentiation by suppressing DNA synthesis in the growth plate and costal chondrocytes (33). TNF-α suppresses DNA synthesis, chondrocyte differentiation and matrix synthesis by unknown mechanisms (41). There are suggestions that TNF-α suppresses Sox-9 expression, a key chondrocyte transcription factor, in inflamed cartilage. Our data suggest that CNP might improve chondrocyte proliferation and differentiation during inflammation by its regulatory effect on Sox-9 expression. Sox9

mRNA expression was up regulated by 5-fold in chondrocytes of $Tg^{Col2a1\text{-}NPPC}$ mice. Sox-9 and CNP are both known to increase the matrix synthesis (42). Although, Sox*9* expression was significantly reduced following TNF-α exposure in $Tg^{Col2a1\text{-}NPPC}$ chondrocytes, it was comparable to the level of expression found in untreated wild-type chondrocytes. Thus, it can be speculated that CNP expression overcomes the effect of pro-inflammatory cytokines on cartilage at the level of transcription factor Sox-9 expression. Sox-9 regulates chondrocyte differentiation, which is not only needed for longitudinal growth, but also for the matrix production that maintains the cartilage integrity.

We also cannot preclude the possibility that CNP overexpression directly modulates the inflammatory response. CNP has been reported to inhibit cytokine-induced leukocyte rolling and to have an anti-platelet/anti-thrombotic effect (43). There are reports that suggest CNP secretion by vascular endothelial cells is increased in response to inflammatory stimuli such as IL-1β, TNF-α and lipopolysaccharide (44, 45). Additionally, CNP suppresses lipopolysaccharide-activated murine macrophage secretion of prostaglandin E2 (46) and inhibits vascular inflammation and intimal hyperplasia in experimental vein grafts (47). Therefore, it is possible that CNP overexpression protects growth and prevents joint damage by diminishing chronic inflammation. Consequently, studies investigating the anti-inflammatory effects of CNP in arthritis models are warranted. While our data demonstrate that linear growth retardation in K/BxN TCR mice can be prevented by CNP overexpression, it remains to be determined whether this protective effect will be observed in other animal models of

inflammation and whether pharmacologic manipulation of the CNP signaling pathway will have similar effects.

Reduction in linear growth is one complication of joint inflammation. Another common complication is widening of the metaphysis, which has been attributed to neovascularization and VEGF overexpression in the growth plate. CNP may play a role in this neovascularization since CNP overexpressing chondrocytes were shown to produce increased levels of VEGF mRNA (Fig. 5) and VEGF immunostaining showed an area that encompass hypertrophic and proliferating chondrocytes, and the trabecular bone where the blood vessels reside (Supplemental Fig. 5). Consequently, $Tg^{Col2a1\text{-}NPPC}$ mice developed widening at the ends of their long bones. We did not observe worsening periarticular overgrowth in the K/BxN TCR; $Tg^{Col2a1\text{-}NPPC}$ mice, perhaps because of the protective effect of CNP overexpression on the chondrocyte response to inflammatory cytokines. However, further studies are needed. An analog of CNP has been shown to improve skeletal growth in mice harboring a knockin *Fgfr3* allele that causes thanatophoric dysplasia in humans (48). It will be interesting to determine whether this analog will be able to lessen the cartilage phenotype in K/BxN TCR mice.

Conclusions:

CNP overexpression by chondrocytes prevented endochondral growth delay and reduced articular cartilage damage in a mouse model of systemic inflammatory arthritis. The likely mechanism for this effect is a cell autonomous increase in chondrocyte differentiation, proliferation, hypertrophy, and matrix production, and a cell autonomous resistance to the growth-suppressive effects of pro-inflammatory cytokines. These data suggest that the CNP/NPR-B pathway may represent a novel therapeutic target to

preserve growth plate and joint cartilage integrity during systemic inflammatory diseases. Although our findings are of particular relevance to JIA, their impact may extend to other forms of inflammatory arthritis and other inflammatory diseases of childhood that stunt longitudinal growth such as inflammatory bowel disease.

References:

1. Chusho H, Tamura N, Ogawa Y, Yasoda A, Suda M, Miyazawa T, et al. Dwarfism and early death in mice lacking C-type natriuretic peptide. Proc Natl Acad Sci U S A 2001;98(7):4016-21.

2. Yasoda A, Komatsu Y, Chusho H, Miyazawa T, Ozasa A, Miura M, et al. Overexpression of CNP in chondrocytes rescues achondroplasia through a MAPK-dependent pathway. Nat Med 2004; 10(1):80-6.

3. Miyazawa T, Ogawa Y, Chusho H, Yasoda A, Tamura N, Komatsu Y, et al. Cyclic GMP-dependent protein kinase II plays a critical role in C-type natriuretic peptide-mediated endochondral ossification. Endocrinology 2002; 143(9):3604-10.

4. Tsuji T, Kunieda T. A loss-of-function mutation in natriuretic peptide receptor 2 (Npr2) gene is responsible for disproportionate dwarfism in cn/cn mouse. J Biol Chem 2005; 280(14):14288-92.

5. Bartels CF, Bukulmez H, Padayatti P, Rhee DK, van Ravenswaaij-Arts C, Pauli RM, et al. Mutations in the transmembrane natriuretic peptide receptor NPR-B impair skeletal growth and cause acromesomelic dysplasia, type Maroteaux. Am J Hum Genet 2004; 75(1):27-34.

6. Olney RC, Bukulmez H, Bartels CF, Prickett TC, Espiner EA, Potter LR, et al. Heterozygous mutations in natriuretic peptide receptor-B (NPR2) are associated with short stature. J Clin Endocrinol Metab 2006; 91(4):1229-32.

7. Bocciardi R, Giorda R, Buttgereit J, Gimelli S, Divizia MT, Beri S, et al. Overexpression of the C-type natriuretic peptide (CNP) is associated with overgrowth and bone anomalies in an individual with balanced t(2;7) translocation. Hum Mutat 2007; 28(7):724-31.

8. Ortoft G, Oxlund H, Jorgensen PH, Andreassen TT. Glucocorticoid treatment or food deprivation counteract the stimulating effect of growth hormone on rat cortical bone strength. Acta Paediatr 1992; 81(11):912-7.

9. Kaufmann S, Jones KL, Wehrenberg WB, Culler FL. Inhibition by prednisone of growth hormone (GH) response to GH-releasing hormone in normal men. J Clin Endocrinol Metab 1988; 67(6):1258-61.

10. White PH. Growth abnormalities in children with juvenile rheumatoid arthritis. Clin Orthop Relat Res 1990(259):46-50.

11. Bacon MC, White PH, Raiten DJ, Craft N, Margolis S, Levander OA, et al. Nutritional status and growth in juvenile rheumatoid arthritis. Semin Arthritis Rheum 1990; 20(2):97-106.

12. Liem JJ, Rosenberg AM. Growth patterns in juvenile rheumatoid arthritis. Clin Exp Rheumatol 2003; 21(5):663-8.

13. MacRae VE, Farquharson C, Ahmed SF. The pathophysiology of the growth plate in juvenile idiopathic arthritis. Rheumatology (Oxford) 2006; 45(1):11-9.

14. Simon D, Lucidarme N, Prieur AM, Ruiz JC, Czernichow P. Treatment of growth failure in juvenile chronic arthritis. Horm Res 2002; 58 Suppl 1:28-32.

15. Takahi K, Hashimoto J, Hayashida K, Shi K, Takano H, Tsuboi H, et al. Early closure of growth plate causes poor growth of long bones in collagen-induced arthritis rats. J Musculoskelet Neuronal Interact 2002; 2(4):344-51.

16. De Benedetti F, Meazza C, Martini A. Role of interleukin-6 in growth failure: an animal model. Horm Res 2002; 58 Suppl 1:24-7.

17. Mangialaio S, Ji H, Korganow AS, Kouskoff V, Benoist C, Mathis D. The arthritogenic T cell receptor and its ligand in a model of spontaneous arthritis. Arthritis Rheum 1999; 42(12):2517-23.

18. Kouskoff V, Korganow AS, Duchatelle V, Degott C, Benoist C, Mathis D. Organ-specific disease provoked by systemic autoimmunity. Cell 1996; 87(5):811-22.

19. Kouskoff V, Korganow AS, Duchatelle V, Degott C, Benoist C, Mathis D. A new mouse model of rheumatoid arthritis: organ-specific disease provoked by systemic autoimmunity. Ryumachi 1997; 37(2):147.

20. Yamada Y, Miyashita T, Savagner P, Horton W, Brown KS, Abramczuk J, et al. Regulation of the collagen II gene in vitro and in transgenic mice. Ann N Y Acad Sci 1990; 580:81-7.

21. Ji H, Gauguier D, Ohmura K, Gonzalez A, Duchatelle V, Danoy P, et al. Genetic influences on the end-stage effector phase of arthritis. J Exp Med 2001; 194(3):321-30.

22. Ji H, Ohmura K, Mahmood U, Lee DM, Hofhuis FM, Boackle SA, et al. Arthritis critically dependent on innate immune system players. Immunity 2002; 16(2):157-68.

23. Ji H, Pettit A, Ohmura K, Ortiz-Lopez A, Duchatelle V, Degott C, et al. Critical roles for interleukin 1 and tumor necrosis factor alpha in antibody-induced arthritis. J Exp Med 2002; 196(1):77-85.

24. Monach P, Hattori K, Huang H, Hyatt E, Morse J, Nguyen L, et al. The K/BxN mouse model of inflammatory arthritis: theory and practice. Methods Mol Med 2007; 136:269-82.

25. Monach PA, Mathis D, Benoist C. The K/BxN arthritis model. Curr Protoc Immunol 2008; Chapter 15: Unit 15 22.

26. Pettit AR, Ji H, von Stechow D, Muller R, Goldring SR, Choi Y, et al. TRANCE/RANKL knockout mice are protected from bone erosion in a serum transfer model of arthritis. Am J Pathol 2001; 159(5):1689-99.

27. Mainil-Varlet P, Aigner T, Brittberg M, Bullough P, Hollander A, Hunziker E, et al. Histological assessment of cartilage repair: a report by the Histology Endpoint Committee of the International Cartilage Repair Society (ICRS). J Bone Joint Surg Am 2003; 85-A Suppl 2:45-57.

28. Gartland A, Mechler J, Mason-Savas A, MacKay CA, Mailhot G, Marks SC, Jr., et al. In vitro chondrocyte differentiation using costochondral chondrocytes as a source of primary rat chondrocyte cultures: an improved isolation and cryopreservation method. Bone 2005; 37(4):530-44.

29. Rasheed Z, Akhtar N, Haqqi TM. Pomegranate extract inhibits the interleukin-1beta-induced activation of MKK-3, p38alpha-MAPK and transcription factor RUNX-2 in human osteoarthritis chondrocytes. Arthritis Res Ther; 12(5):R195.

30. Ahmed S, Wang N, Lalonde M, Goldberg VM, Haqqi TM. Green tea polyphenol epigallocatechin-3-gallate (EGCG) differentially inhibits interleukin-1 beta-induced expression of matrix metalloproteinase-1 and -13 in human chondrocytes. J Pharmacol Exp Ther 2004; 308(2):767-73.

31. Singh R, Ahmed S, Malemud CJ, Goldberg VM, Haqqi TM. Epigallocatechin-3-gallate selectively inhibits interleukin-1beta-induced activation of mitogen activated protein kinase subgroup c-Jun N-terminal kinase in human osteoarthritis chondrocytes. J Orthop Res 2003; 21(1):102-9.

32. Agoston H, Khan S, James CG, Gillespie JR, Serra R, Stanton LA, et al. C-type natriuretic peptide regulates endochondral bone growth through p38 MAP kinase-dependent and -independent pathways. BMC Dev Biol 2007; 7:18.

33. Murakami S, Lefebvre V, de Crombrugghe B. Potent inhibition of the master chondrogenic factor Sox9 gene by interleukin-1 and tumor necrosis factor-alpha. J Biol Chem 2000; 275(5):3687-92.

34. Akiyama H, Chaboissier MC, Martin JF, Schedl A, de Crombrugghe B. The transcription factor Sox9 has essential roles in successive steps of the chondrocyte differentiation pathway and is required for expression of Sox5 and Sox6. Genes Dev 2002; 16(21):2813-28.

35. Akiyama H, Kim JE, Nakashima K, Balmes G, Iwai N, Deng JM, et al. Osteo-chondroprogenitor cells are derived from Sox9 expressing precursors. Proc Natl Acad Sci U S A 2005; 102(41):14665-70.

36. De Benedetti F, Massa M, Pignatti P, Albani S, Novick D, Martini A. Serum soluble interleukin 6 (IL-6) receptor and IL-6/soluble IL-6 receptor complex in systemic juvenile rheumatoid arthritis. Journal of Clinical Investigation 1994; 93(5):2114-9.

37. Manghe H. Serum cytokines in juvenile rheumatoid arthritis. Correlation with conventional inflammation parameters and clinical subtypes. Arthritis and Rheumatism 1995; 38:211-220.

38. MacRae VE, Farquharson C, Ahmed SF. The restricted potential for recovery of growth plate chondrogenesis and longitudinal bone growth following exposure to pro-inflammatory cytokines. J Endocrinol 2006;189(2):319-28.

39. Zwerina J, Hayer S, Redlich K, Bobacz K, Kollias G, Smolen JS, et al. Activation of p38 MAPK is a key step in tumor necrosis factor-mediated inflammatory bone destruction. Arthritis Rheum 2006; 54(2):463-72.

40. Olney RC. C-type natriuretic peptide in growth: a new paradigm. Growth Horm IGF Res 2006; 16 Suppl A: S6-14.

41. Klooster AR, Bernier SM. Tumor necrosis factor alpha and epidermal growth factor act additively to inhibit matrix gene expression by chondrocyte. Arthritis Res Ther 2005; 7(1):R127-38.

42. Pejchalova K, Krejci P, Wilcox WR. C-natriuretic peptide: an important regulator of cartilage. Mol Genet Metab 2007; 92(3):210-5.

43. Scotland RS, Cohen M, Foster P, Lovell M, Mathur A, Ahluwalia A, et al. C-type natriuretic peptide inhibits leukocyte recruitment and platelet-leukocyte interactions via suppression of P-selectin expression. Proc Natl Acad Sci U S A 2005; 102(40):14452-7.

44. Suga S, Itoh H, Komatsu Y, Ogawa Y, Hama N, Yoshimasa T, et al. Cytokine-induced C-type natriuretic peptide (CNP) secretion from vascular endothelial cells--evidence for CNP as a novel autocrine/paracrine regulator from endothelial cells. Endocrinology 1993; 133(6):3038-41.

45. Scotland RS, Ahluwalia A, Hobbs AJ. C-type natriuretic peptide in vascular physiology and disease. Pharmacol Ther 2005; 105(2):85-93.

46. Kiemer AK, Lehner MD, Hartung T, Vollmar AM. Inhibition of cyclooxygenase-2 by natriuretic peptides. Endocrinology 2002; 143(3):846-52.

47. Schachner T, Zou Y, Oberhuber A, Mairinger T, Tzankov A, Laufer G, et al. Perivascular application of C-type natriuretic peptide attenuates neointimal hyperplasia in experimental vein grafts. Eur J Cardiothorac Surg 2004; 25(4):585-90.

48. Lorget F, Kaci N, Peng J, Benoist-Lasselin C, Mugniery E, Oppeneer T, et al. Evaluation of the therapeutic potential of a CNP analog in a Fgfr3 mouse model recapitulating achondroplasia. Am J Hum Genet; 91(6):1108-14.

Figure Legends

Figure 1:

$Tg^{Col2a1\text{-}NPPC}$ (TG) mice show longitudinal overgrowth

Photograph (A) and radiographs (B) of 24-week-old non-transgenic (WT) and $Tg^{Col2a1\text{-}NPPC}$ CNP overexpressing (TG) female littermates. (C) Photomicrographs of Safranin-O/Fast Green stained proximal tibia growth plates from 13-week-old female WT and TG mice. Measurements are shown with vertical blue lines in the growth plates. (D) Graph depicting the diameter of hypertrophic chondrocytes in WT and TG and mice at 1 (n=3, 4), 3 (n=4, 6), and 4 (n=4, 5) weeks of age. (E) Graph depicting linear growth in WT and TG mice at 6 (n=12, 16), 9 (n=6, 10), 11 (n=16, 9), 13 (n=6, 8), 15 (n=8, 12), 20 (n=9, 6), and 26 (n=9, 6) weeks of age (male and female combined). (F) Graph depicting the percent of growth plate chondrocytes that incorporated BrdU in 1 (n=4, 5), 2.5 (n=2, 4) and 3.5 (n=5, 5) week-old WT and TG mice. (G) Photomicrographs of growth plate and

(H) articular cartilage from 4-week-old WT and TG mice following Hoechst staining of cell nuclei (upper) and *in situ* hybridization using an anti-sense *NPPC* probe (lower). Brackets show the growth plate width. Arrows point to growth plate chondrocytes (G) and to articular chondrocytes in (H). Means ± S.D. are shown in all graphs.

Figure 2: K/BxN TCR mice have growth retardation and cartilage damage

(A) Photograph of 12-week-old female K/BxN mice with (K/BxN TCR) and without (BXN) the TCR transgene. Compared with the BXN mouse, the K/BxN TCR (indicated by K/BxN in all panels) mouse is smaller and has evidence of inflammatory arthritis; arrows point to the hind paw, which is swollen in the K/BxN TCR mouse. (B) Graph depicting the linear growth of BXN and K/BxN TCR mice (males and females combined). Statistical analysis showed significant differences between BxN and K/BxN TCR mice at 4 (n=12, 10), 8 (n=15, 8), 10 (n=16, 8) and 14 (n=14, 5) weeks of age (male and female combined) ($p<0.05$, F test). (C) Photomicrograph of hematoxylin and eosin stained proximal tibia growth plate cartilage from 9-week-old female K/BxN TCR and BXN littermates, at 40x magnification. D) Photomicrographs of sagittal sections through the femoro-tibial joint of 9-week-old female BXN and K/BxN TCR littermates stained with hematoxylin and eosin. E) Photomicrographs of coronal sections through the femoro-tibial joint of 12-week-old female BXN and K/BxN TCR littermates stained with Safranin-O. K/BxN TCR mice exhibit chondrocyte loss (arrows), cartilage thinning (black lines), and reduced proteoglycan content compared to BXN mice.

Figure 3: CNP overexpression reduces growth retardation in K/BxN TCR mice

(A) Breeding strategy to generate K/BxN TCR mice that overexpress CNP in chondrocytes. Grey coat color segregates with the KRN TCR transgene (25).

(B) K/BxN; $Tg^{Col2a1\text{-}NPPC}$ mice develop arthritis but not growth retardation. Nose-to-tail tip lengths of K/BxN TCR; $Tg^{Col2a1\text{-}NPPC}$ and K/BxN TCR mice are shown. Male and female mice were pooled for the graph. Statistical analysis showed significant difference between K/BxN and K/BxN TCR/$Tg^{Col2a1\text{-}NPPC}$ mice at 10 (n=16, 6), 13 (n=7, 5), 15 (n=14, 6), 20 (n=7, 5) and 26 (n=7, 5) weeks of age ($p<0.05$, F test).

(C) Hematoxylin and eosin stained coronal sections of proximal tibia growth plates of 12-week-old a) non-transgenic (BxN), b) arthritic (K/BxN), c) arthritic and CNP overexpressing (K/BxN; $Tg^{Col2a1\text{-}NPPC}$) mice and d) CNP overexpressing ($Tg^{Col2a1\text{-}NPPC}$) (20X magnification).

(D) Radiographs of lower extremities of 12-week-old male K/BxN mice with (+) and without (-) the $Tg^{Col2a1\text{-}NPPC}$ and/or the TCR transgene. The length of each tibia is indicated.

(E) Histologically-determined inflammation scores (left), ICRS system II scores (middle), ICRS system III scores (right) in arthritic mice with (K/BxN; $Tg^{Col2a1\text{-}NPPC}$) and without (K/BxN) CNP overexpression. All graphs depict mean $\pm$ 1 SD. * = $p < 0.05$

Figure 4: CNP overexpression lessens cartilage damage in K/BxN TCR mice

(A, B) Photomicrographs of H&E stained sagittal sections across the femoro-tibial joint of 13-week-old male non-transgenic (BxN), arthritic (K/BxN) CNP overexpressing ($Tg^{Col2a1\text{-}NPPC}$), and arthritic and CNP overexpressing (K/BxN; $Tg^{Col2a1\text{-}NPPC}$) mice. Arrows indicate femoral articular cartilage. Images are taken from the mice within each genotypic group that had the median score for histological severity. (A) panels are at 10x magnification, while (B) panels are at 40x magnification. (C) Photomicrographs of Safranin-O stained coronal sections across the femoro-tibial joint of 12-week-old female

mice. Arrows indicate the cartilage surface of the tibia plateau. (D) Photomicrographs of H&E stained sagittal sections across the femoro-tibial joint of 12-week-old female non-transgenic (BxN), arthritic (K/BxN), and arthritic and CNP overexpressing (K/BxN;$Tg^{Col2a1\text{-}NPPC}$) mice. Although K/BxN; $Tg^{Col2a1\text{-}NPPC}$ mice have pannus and synovial inflammation (solid arrows) there is less damage to the articular cartilage surface (dashed arrows).

Figure 5: CNP overexpression in chondrocytes increases the expression of mRNAs associated with cartilage anabolism

Quantitative RT-PCR results obtained from primary chondrocyte cultures recovered from $Tg^{Col2a1\text{-}NPPC}$ and wild-type (WT) mice for several mRNAs associated with cartilage growth. * depicts significance, $p < 0.05$).

Figure 6: CNP overexpression in chondrocytes dampens the response to inflammatory cytokines

(A) Graph depicting relative levels of mRNA expression for *Npr2* (normalized to levels in wild-type primary chondrocyte) for primary cultures obtained from non-transgenic and $Tg^{Col2a1\text{-}NPPC}$ mice without or following exposure to TNF-α (10 ng/ml) and IL-1β (10 ng/ml).

(B) Western blot analysis of Erk1 (p44) and p38 MAPK phosphorylation.

Upper panels: Erk1 phosphorylation was inhibited by the CNP transgene. TNF-α treatment increased Erk1 (p44) phosphorylation even in CNP transgenic mouse chondrocytes but IL-1β did not change suppression of Erk1 (p44) phosphorylation in $Tg^{Col2a1\text{-}NPPC}$ chondrocytes.

Lower panels: Phosphorylation of p38 MAPK was increased in $Tg^{Col2a1\text{-}NPPC}$ transgenic mouse cartilage as compared to non-transgenic littermates. Overnight TNF-α and IL-1β treatments significantly increased the p38 phosphorylation in non-transgenic chondrocytes while this effect was only modest in the $Tg^{Col2a1\text{-}NPPC}$ mice.

(C) Quantitative RT-PCR of matrix metalloproteinase (MMP) -3, -9 and -13 in primary chondrocytes isolated from rib cages of WT and $Tg^{Col2a1\text{-}NPPC}$ mice.

(D) Quantitative RT-PCR of Sox-9 transcription factor in primary chondrocytes isolated from rib cages of WT and $Tg^{Col2a1\text{-}NPPC}$ mice.

Supplemental tables and figures:

Table S1: Clinical Arthritis Scoring

Scores of mild (1), moderate (2) and severe (3) were given in three different clinical categories: ***Severity of arthritis***, (1) the foot remains in its original V shape, (2) disappearance of the V shape and mild ankle swelling and (3) inversion of the V shape by expansion of the ankle and hind foot greater than the width of the forefoot swelling. All 4 limb scores were added to obtain a total score of up to 12 points. Then a score for ***severity of affected joint mobility*** (Range of Motion; ROM) was given, with scores of (1) mild difficulty in ROM, (2) moderate difficulty in ROM, or (3) complete immobility.

3) A score for the ***severity of erythema*** in hind paws, with (1) mild, (2) moderate, and (3) severe, were also added to the scores of severity of arthritis to obtain maximum score of 18. Higher scores represent more severe arthritis.

Also, hind paw ankle thickness between the anterior and posterior surfaces of the ankle joints was measured using a caliper at 3 weeks of age and at the time of sacrifice.

Table S2: International Cartilage Repair Society (ICRS) Visual Histology Score (2003)

In order to assess cartilage damage and repair during inflammatory arthritis a visual histology scoring system was used based on ICRS criteria. Regularity of the surface of the articular cartilage, matrix staining, distribution and cluster patterns of the chondrocyte populations, subchondral bone structure and cartilage mineralization were assessed (27). In the ICRS system, lower scores represent cartilage damage or poor cartilage homeostasis.

Table S3: Nose-to-tail tip length measurements of $Tg^{Col2a1\text{-}NPPC}$ and WT mice

Nose-to-tail tip length measurements of 4.5-weeks-old CNP transgenic ($Tg^{Col2a1\text{-}NPPC}$) and WT mice were statistically significant. n: Number of mice studied in each group.

Figure S1: Scatter plot of body lengths (nose-tail-tip) and arthritis

Scatter plot of nose-to-tail lengths and arthritis scores in 13.5-week-old male and female K/BxN TCR mice (n=10). Line demonstrated the negative correlation between the arthritis scores and the nose-to-tail tip length of the arthritic mice.

Figure S2: CNP overexpression reduces growth retardation in K/BxN TCR mice

A: $K/BxN/Tg^{Col2a1\text{-}NPPC}$ (n=2) mice have wider proximal tibia growth plates as compared to the K/BxN (TCR) (n=3) mice that do not overexpress CNP. Asterix indicates statistical significance between groups.

B: Mean percent BrdU positive cells of proximal tibia growth plates are significantly higher in the $K/BxN/Tg^{Col2a1\text{-}NPPC}$ mice. Asterisk indicates statistical significance between groups.

Figure S3: Western blot analysis of NPR-B in primary chondrocyte cultures after cytokine treatment

Immunodetection of NPR-B in cell extracts from $Tg^{Col2a1\text{-}NPPC}$ (+) and wild type ($Tg^{Col2a1\text{-}NPPC}$ (-)) primary chondrocytes following exposure to inflammatory cytokines.

Figure S4: VEGF immunostaining

VEGF immunostaining on growth plates of 7-week-old male littermates: A) Wild type (WT) and B) $Tg^{Col2a1\text{-}NPPC}$ littermates' growth plates stained with VEGF-A (Santa Cruz®). Localization of VEGF (brown stained areas) was mainly on the pre-hypertrophic chondrocytes (arrows) and beneath the hypertrophic chondrocyte area in WT (shown with bracket). In $Tg^{Col2a1\text{-}NPPC}$ mice it encompassed the area between the pre-hypertrophic and hypertrophic chondrocytes and further extended into the trabecular bone where blood vessels reside (shown with bracket). The staining was most remarkable in the $Tg^{Col2a1\text{-}NPPC}$ as compared to wild type littermates.

Figure S5: Igf1, Igf1r, Igfbp3 mRNA expression levels in wild type and $Tg^{Col2a1\text{-}NPPC}$ mice before and after cytokine treatment

RT-PCR showed no significant difference between the wild type (WT) and $Tg^{Col2a1\text{-}NPPC}$ mice chondrocytes *Igf1* and *Igf1r* expression while *Igfbp3* levels were significantly elevated in $Tg^{Col2a1\text{-}NPPC}$ chondrocytes.

We observed suppression of *Igf1 and Igf1r* expression after both TNF-α and IL-1β treatment but no significant change in the Igfbp3 expression in WT chondrocytes. Similarly both *Igf1 and Igf1r* expression were tapered after TNF-α and IL-1β treatment of $Tg^{Col2a1\text{-}NPPC}$ chondrocytes. However, *Igfbp3* levels were significantly increased in $Tg^{Col2a1\text{-}NPPC}$ chondrocytes after both cytokine treatments.

Abbreviations:

CNP: C-type natriuretic peptide

IGF1: Insulin-like growth factor 1

IGF1R: Insulin-like growth factor 1 receptor

IGFBP3: Insulin-like growth factor-binding protein 3

FGFR3: Fibroblast growth factor receptor 3

$Tg^{Col2a1\text{-}NPPC}$: Human CNP cDNA (NPPC) overexpressing mouse under Col2a1 mouse promoter gene

JIA: Juvenile inflammatory arthritis

IL-1β: Interleukin 1 beta

K/BxN TCR: systemic inflammatory arthritis mouse model.

K/BxN: K/BxN TCR

MMP: Matrix metalloproteinases

NPR-B: Natriuretic peptide receptor B

NTG: Non-transgenic mouse

RA: Rheumatoid arthritis

RT-PCR: Real-time PCR

Tgf-β: Transforming growth factor beta

TCR: T-cell receptor

TNF-α: Tumor necrosis factor alpha

Vegf; Vascular endothelial growth factor

Competing interests:

The authors declare that they have no competing interests.

Authors' contributions:

HB designed the study, acquired, analyzed, and interpreted the data, and drafted the manuscript. FK contributed to the acquisition of data and carried out western blots and RT-PCR. CB contributed to the development of the CNP transgenic mice and critically reviewed the draft. SM contributed to the design of the primary chondrocyte experiments and critically reviewed and helped write the first draft of the manuscript. AOL helped with the K/BxN TCR mice. AS performed the statistics. TMH contributed to the interpretation of the data and supervised the *in vitro* assays reported in the manuscript, and critically reviewed the draft. MLW contributed to the discussions of the design of the study, supervised the CNP transgenic mouse development, and critically reviewed and revised the manuscript. All authors approved the submitted version of the manuscript.

Authors' information:

Hülya Bükülmez, MD is an Assistant Professor of Pediatrics in the Department of Pediatrics at MetroHealth Medical Center, Case Western Reserve University School of Medicine, Cleveland, OH. She also holds a joint appointment in the Skeletal Research Center, Department of Biology, College of Arts and Sciences, Case Western Reserve University.

Fozia Khan, Ph.D. was a Post Doctoral fellow in the Department of Genetics, Case Western Reserve University School of Medicine. Her current position is at Community Health Sciences, College of Applied Medical Sciences, King Saud University, Riyadh, KSA,

Cynthia F. Bartels is a Research Assistant in the Department of Genetics, Case Western Reserve University School of Medicine, Cleveland, OH.

Shunichi Murakami, MD, Ph.D. is an Assistant Professor in the Department of Orthopaedics, Case Western Reserve University School of Medicine, Cleveland, OH.

Adriana Ortiz-Lopez, Ph.D., is a post doctoral fellow in the Section on Immunology and Immunogenetics, Joslin Diabetes Center, Harvard Medical School, Boston, MA.

Abdus Sattar, PhD., is a biostatistician at the Case Western Reserve University School of Medicine, Cleveland, OH.

Tariq M. Haqqi, Ph.D., is the Director of Research Laboratories in the Department of Medicine/Rheumatology, MetroHealth Medical Center, Case Western Reserve University, Cleveland, OH.

Matthew L. Warman, MD is an Investigator with the Howard Hughes Medical Institute and Director of the Orthopaedic Research Laboratories at Children's Hospital, Boston, and Professor of Genetics and Orthopaedic Surgery at Harvard Medical School, Boston, MA.

Acknowledgement:

The authors thank Diana Mathis, Ph.D. and Christophe Benoist, Ph.D. from the Section on Immunology and Immunogenetics, Joslin Diabetes Center, Harvard Medical School, Boston, MA for the generous gift of K/BxN TCR mice.

The Col2a1 promoter and enhancer construct was a gift from Yoshihiko Yamada, Ph.D. Molecular Biology Section, National Institute of Dental and Craniofacial Research, National Institute of Health. The authors thank Dr. Yamada for his contribution.

Several experiments were performed at the Skeletal Research Center in the laboratories of Arnold Caplan, PhD., who discussed study results and helped interpret data. Dr. Caplan also critically reviewed the manuscript. The authors are grateful for Dr. Caplan's input on the study.

Jean F. Welter, MD, PhD., generously helped score joint cartilage of the mice, reviewed the data, and helped with the manuscript.

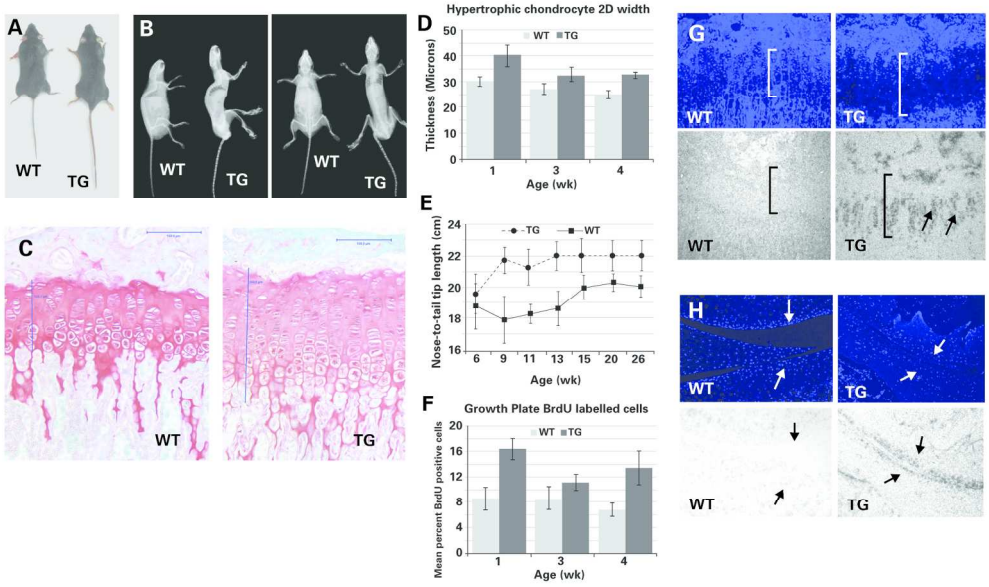

Figure1: Tg (TG) mice show longitudinal overgrowth

Photograph (A) and radiographs (B) of 24-week-old non-transgenic (WT) and Tg CNP overexpressing (TG) female littermates. (C) Photomicrographs of Safranin-O/Fast Green stained proximal tibial growth plates from 13-week-old female WT and TG mice. Measurements are shown with vertical blue lines in the growth plates. (D) Graph depicting the diameter of hypertrophic chondrocytes in WT and TG and mice at 1 (n=3, 4), 3 (n=4, 6), and 4 (n=4, 5) weeks of age. (E) Graph depicting linear growth in WT and TG mice at 6 (n=12, 16), 9 (n=6, 10), 11 (n=16, 9), 13 (n=6, 8), 15 (n=8,12), 20 (n=9, 6), and 26 (n=9, 6) weeks of age (male and female combined). (F) Graph depicting the percent of growth plate chondrocytes that incorporated BrdU in 1 (n=4, 5), 2.5 (n=2, 4) and 3.5 (n=5, 5) week-old WT and TG mice. (G) Photomicrographs of growth plate and (H) articular cartilage from 4-week-old WT and TG mice following Hoechst staining of cell nuclei (upper) and in situ hybridization using an anti-sense NPPC probe (lower). Brackets show the growth plate width. Arrows point to growth plate chondrocytes (G) and to articular chondrocytes in (H). Means ± S.D. are shown in all graphs.

177x107mm (300 x 300 DPI)

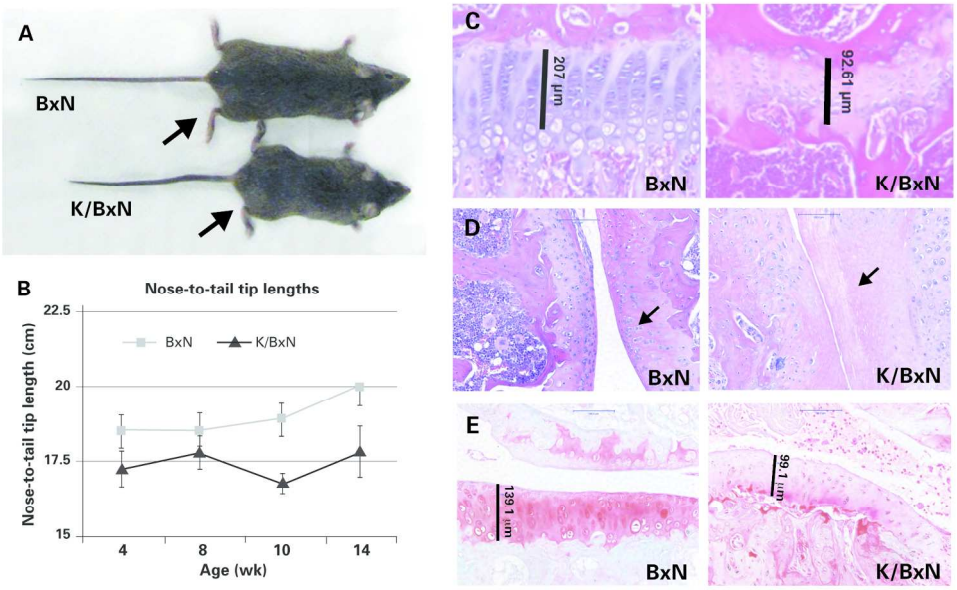

Figure 2: K/BxN TCR mice have growth retardation and cartilage damage.
(A) Photograph of 12-week-old female K/BxN mice with (K/BxN TCR) and without (BXN) the TCR transgene. Compared with the BXN mouse, the K/BxN TCR (indicated by K/BxN in all panels) mouse is smaller and has evidence of inflammatory arthritis; arrows point to the hind paw, which is swollen in the K/BxN TCR mouse. (B) Graph depicting the linear growth of BXN and K/BxN TCR mice (males and females combined). Statistical analysis showed significant differences between BxN and K/BxN TCR mice at 4 (n=12, 10), 8 (n=15, 8), 10 (n=16, 8) and 14 (n=14, 5) weeks of age (male and female combined) ($p<0.05$, F test). (C) Photomicrograph of hematoxylin and eosin stained proximal tibia growth plate cartilage from 9-week-old female K/BxN TCR and BXN littermates, at 40x magnification. D) Photomicrographs of sagittal sections through the femoral-tibial joint of 9-week-old female BXN and K/BxN TCR littermates stained with hematoxylin and eosin. E) Photomicrographs of coronal sections through the femoral-tibial joint of 12-week-old female BXN and K/BxN TCR littermates stained with Safranin-O. K/BxN TCR mice exhibit chondrocyte loss (arrows), cartilage thinning (black lines), and reduced proteoglycan content compared to BXN mice.

177x114mm (300 x 300 DPI)

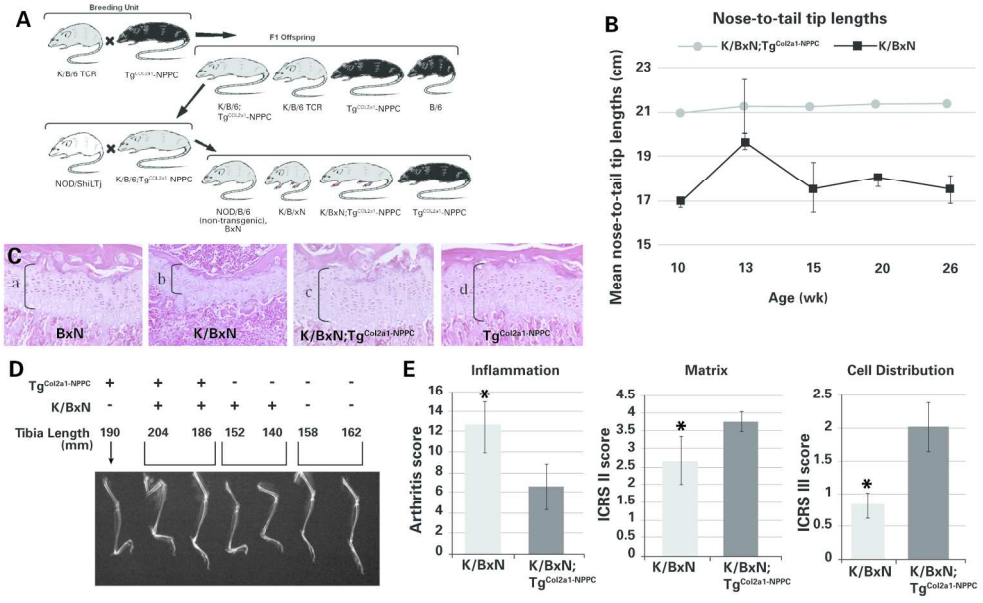

Figure 3: CNP overexpression reduces growth retardation in K/BxN TCR mice.

(A) Breeding strategy to generate K/BxN TCR mice that overexpress CNP in chondrocytes. Grey coat color segregates with the KRN TCR transgene (25).

(B) K/BxN; Tgmice develop arthritis but not growth retardation. Nose-to-tail tip lengths of K/BxN TCR; Tgand K/BxN TCR mice are shown. Male and female mice were pooled for the graph. Statistical analysis showed significant difference between K/BxN and K/BxN TCR/Tg mice at 10 (n=16, 6), 13 (n=7, 5), 15 (n=14, 6), 20 (n=7, 5) and 26 (n=7, 5) weeks of age ($p<0.05$, F test).

(C) Hematoxylin and eosin stained coronal sections of proximal tibia growth plates of 12-week-old a) non-transgenic (BxN), b) arthritic (K/BxN), c) arthritic and CNP overexpressing (K/BxN; Tg) mice and d) CNP overexpressing () (20X magnification).

(D) Radiographs of lower extremities of 12-week-old male K/BxN mice with (+) and without (-) the Tgand/or the TCR transgene. The length of each tibia is indicated.

(E) Histologically-determined inflammation scores (left), ICRS system II scores (middle), ICRS system III scores (right) in arthritic mice with (K/BxN; Tg) and without (K/BxN) CNP overexpression. All graphs depict mean ± 1 SD. * = $p < 0.05$

177x114mm (300 x 300 DPI)

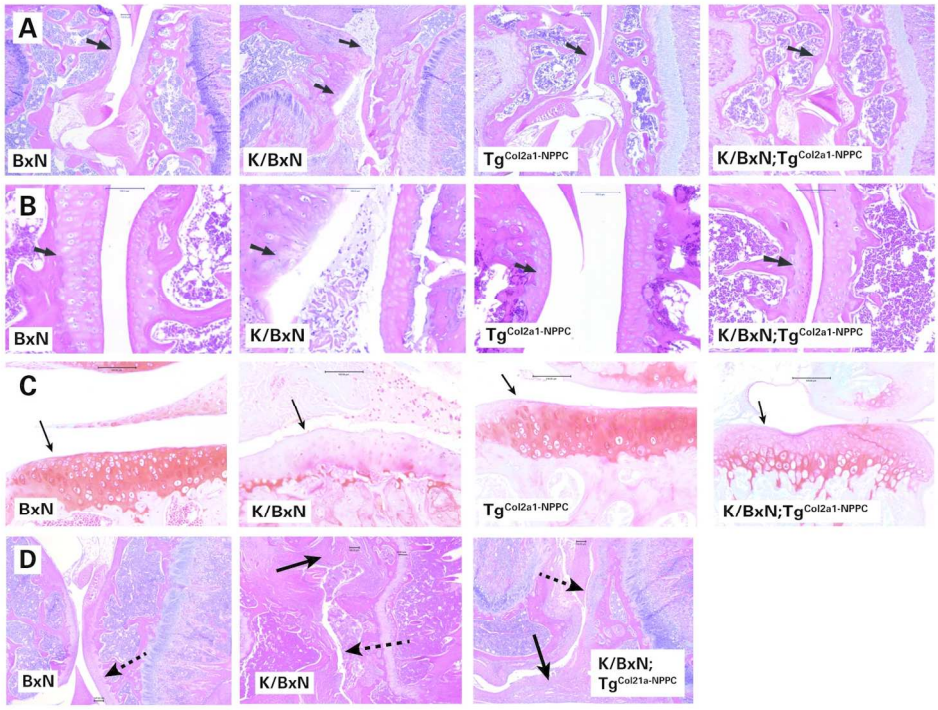

Figure 4: CNP overexpression lessens cartilage damage in K/BxN TCR mice

(A, B) Photomicrographs of H&E stained sagittal sections across the femoro-tibial joint of 13-week-old male non-transgenic (BxN), arthritic (K/BxN) CNP overexpressing (Tg), and arthritic and CNP overexpressing (K/BxN;Tg) mice. Arrows indicate femoral articular cartilage. Images are taken from the mice within each genotypic group that had the median score for histological severity. (A) panels are at 10x magnification, while (B) panels are at 40x magnification. (C) Photomicrographs of Safranin-O stained coronal sections across the femoro-tibial joint of 12-week-old female mice. Arrows indicate the cartilage surface of the tibial plateau. (D) Photomicrographs of H&E stained sagittal sections across the femoro-tibial joint of 12-week-old female non-transgenic (BxN), arthritic (K/BxN), and arthritic and CNP overexpressing (K/BxN;Tg) mice. Although K/BxN; Tgmice have pannus and synovial inflammation (solid arrows) there is less damage to the articular cartilage surface (dashed arrows).

152x114mm (300 x 300 DPI)

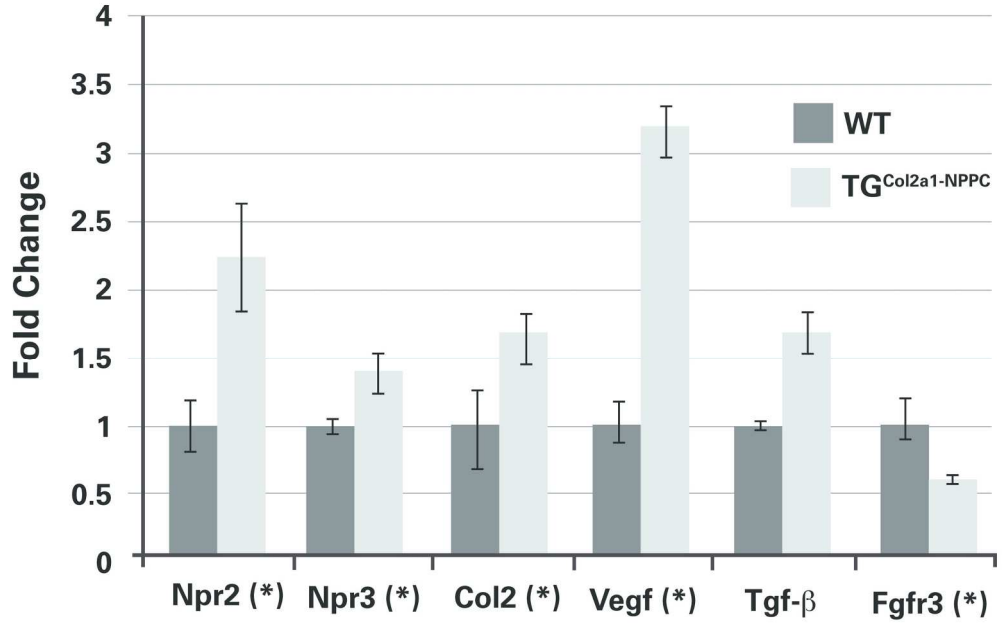

Figure 5: CNP overexpression in chondrocytes increases the expression of mRNAs associated with cartilage anabolism. Quantitative RT-PCR results obtained from primary chondrocyte cultures recovered from Tg and wild-type (WT) mice for several mRNAs associated with cartilage growth. * depicts significance, $p < 0.05$).

190x127mm (300 x 300 DPI)

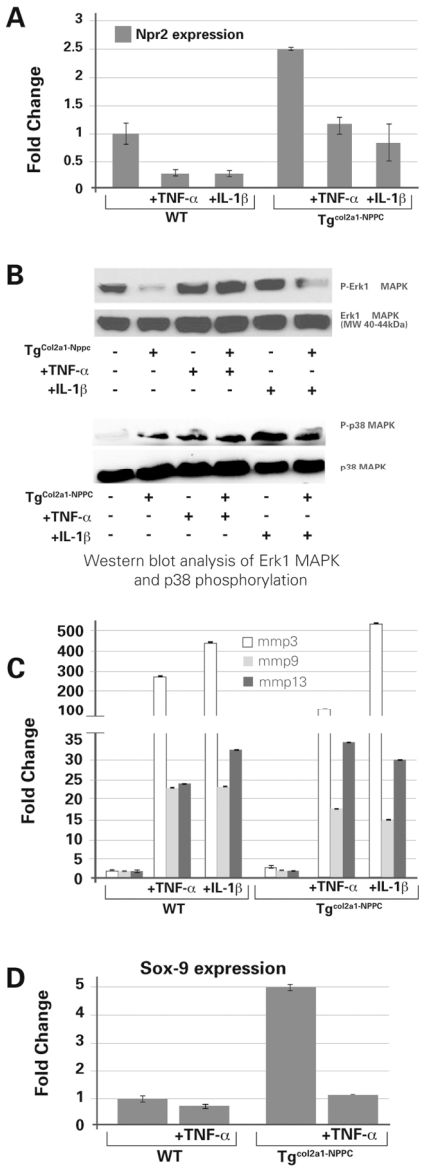

Figure 6: CNP overexpression in chondrocytes dampens the response to inflammatory cytokines.
(A) Graph depicting relative levels of mRNA expression for Npr2 (normalized to levels in wild-type primary chondrocyte) for primary cultures obtained from non-transgenic and TgCol2a1-NPPC mice without or following exposure to TNF-α (10 ng/ml) and IL-1β (10 ng/ml).
(B) Western blot analysis of Erk1 (p44) and p38 MAPK phosphorylation.
Upper panels: Erk1 phosphorylation was inhibited by the CNP transgene. TNF-α treatment increased Erk1 (p44) phosphorylation even in CNP transgenic mouse chondrocytes but IL-1β did not change suppression of Erk1 (p44) phosphorylation in Tg chondrocytes.
Lower panels: Phosphorylation of p38 MAPK was increased in Tgtransgenic mouse cartilage as compared to non-transgenic littermates. Overnight TNF-α and IL-1β treatments significantly increased the p38 phosphorylation in non-transgenic chondrocytes while this effect was only modest in the Tgmice.
(C) Quantitative RT-PCR of matrix metalloproteinase (MMP) -3, -9 and -13 in primary chondrocytes isolated from rib cages of WT and Tgmice.
(D) Quantitative RT-PCR of Sox-9 transcription factor in primary chondrocytes isolated from rib cages of WT and Tg mice.